
Significantly accelerated osteoblast cell growth on aligned TiO₂ nanotubes

Seunghan Oh, Chiara Daraio, Li-Han Chen, Thomas R. Pisanic, Rita R. Fiñones, Sungho Jin

Materials Sciences and Engineering program, Department of Mechanical Aerospace Engineering, University of California at San Diego, La Jolla, California 92093-0411

Received 12 August 2005; revised 8 December 2005; accepted 22 December 2005

Published online 6 April 2006 in Wiley InterScience (www.interscience.wiley.com). DOI: 10.1002/jbm.a.30722

Abstract: Vertically aligned yet laterally spaced nanoscale TiO₂ nanotubes have been grown on Ti by anodization, and the growth of MC3T3-E1 osteoblast cells on such nanotubes has been investigated. The adhesion/propagation of the osteoblast is substantially improved by the topography of the TiO₂ nanotubes with the filopodia of growing cells actually going into the nanotube pores, producing an inter-

locked cell structure. The presence of the nanotube structure induced a significant acceleration in the growth rate of osteoblast cells by as much as ~300–400%. © 2006 Wiley Periodicals, Inc. *J Biomed Mater Res* 78A: 97–103, 2006

Key words: TiO₂ nanotubes; osteoblast cell; adhesion; accelerated cell growth

INTRODUCTION

Titanium (Ti) and its alloys have been widely used as implantation materials that can provide direct physical bonding with adjacent bone surface without forming a fibrous tissue interface layer (osseo-integrate) in orthopedic and dental surgery.^{1–3} The initial interaction between a metal implant and a growing bone plays an important role in fabricating prostheses for load-bearing applications.^{4,5} While pure Ti metal lacks desirable bioactive (bone-growth) properties, a thin TiO₂ passivation layer forms on Ti surface to impart bioactivity and chemical bonding to bone.⁶ Such a layer, however, is composed of smooth and dense TiO₂ and is susceptible to the formation of fibrous tissue that prohibits osteoblastic cells from firmly attaching onto the surface, and can cause the loosening of implant and inflammation.⁷

Coating of bioactive materials such as hydroxyapatite and calcium phosphate on Ti surface is a commonly used technique to make the Ti surface more bioactive.^{8–13} The fatal drawback of these currently available coating techniques is that such a flat and continuous coatings tend to fail by fracture or delamination at the interface between the implant and the bone.¹⁴ It would thus be desirable if the interface is bonded with an improved and integrated structure,

for example, with a interlocked configuration with a much increased adhesion area, and as a discrete, less continuous layer to minimize interface stress and delamination. In this article, we report on design of such an improved and nanoscale interface structure on Ti implant metal surface, and that such a structure also induces a significant acceleration of cell growth.

Recently, Webster et al. reported that the bioactivity and osteoblast (bone-forming cell) adhesion on nanograined sintered ceramics of alumina or titania improved by as much as 20–30% as compared with large-grain size ceramics.^{15,16} Adhesion of cells such as osteoblast is a crucial prerequisite to subsequent cell functions such as synthesis of extracellular matrix proteins, formation of mineral deposits, and osseo-integration on the substrate surface. TiO₂-type nanostructures have received considerable attention in recent years, as they exhibit strong photocatalytic properties, which can be useful for environmental purifications and solar cell type applications. Nanotube-shaped TiO₂ has also been fabricated by various techniques such as sol-gel synthesis, electrochemical deposition, and anodization.^{17–19} In our recent research,²⁰ we demonstrated that chemically treated TiO₂ nanotubes induced a formation of nanosized sodium titanate and hydroxyapatite with a significantly (by seven-fold) accelerated kinetics. The purpose of this work is to study *in vitro* behavior of osteoblast cells cultured on vertically aligned TiO₂ nanotubes and investigate the effect of such nanostructure on osteoblast cell morphology and kinetics of cell proliferation. Such an

Correspondence to: S. Jin; e-mail: jin@ucsd.edu
Contract grant sponsor: K. Iwama Endowed Chair Fund

accelerated cell growth is beneficial for faster cure of dental and orthopaedic patients, as well as for a variety of biomedical diagnostic and therapeutic applications.

MATERIALS AND METHODS

Materials

A layer of vertically aligned TiO₂ nanotubes on Ti metal surface was fabricated by anodization technique.²⁰ For cell adhesion studies, MC3T3-E1 mouse osteoblast cells (CRL-2593, sub-clone 4, ATCC, Rockville, MD) were used.

TiO₂ nanotubes fabrication

A Ti sheet (0.25 mm thick, 99.5%, Alfa-Aesar, Ward Hill, MA) was chemically cleaned for 5 min in 5.5 M of HNO₃ with a few drops of hydrofluoric acid (HF; ACS grade, Fisher Scientific, Pittsburg, PA), rinsed in distilled water, and dried at 60°C. TiO₂ nanotubes were prepared by anodization in a 0.5% HF solution at 20 V for 30 min at room temperature. A platinum electrode (thickness, 0.1 mm; purity, 99.99%; Alfa Aesar, Ward Hill, MA) was used as the cathode. To crystallize the as-deposited amorphous-structured TiO₂ nanotubes, the specimens were heat-treated at 500°C for 2 h. All the experimental specimens (0.5 × 0.5 cm²) used for cell adhesion assays were sterilized by autoclaving. A pure Ti sheet was polished by SiC emery paper (No. 600 grit size) for use as a control group sample.

Osteoblast cell culture

Each 1 mL of cells was mixed with 10 mL of alpha-minimum essential medium (α-MEM) in the presence of 10% fetal bovine serum (FBS) and 1% penicillin-streptomycin (PS). The cell suspension was plated in a cell culture dish and incubated under 37°C, 5% CO₂ environment. When the concentration of the MC3T3-E1 osteoblastic cells reached ~3 × 10⁵ cells/mL, they were seeded onto the experimental substrate of interest (TiO₂ or Ti), which were then placed on a 12-well polystyrene plate, and stored in a CO₂ incubator for 2, 12, 24, or 48 h to observe cell morphology and count viable attached cells as a function of incubation time. The concentration of the cells seeded onto the specimen substrate was ~1.0 × 10⁵ cells/well.

Cell observation and cell viability assay by electron microscope

After the selected incubation period, the samples were washed with 0.1M phosphate buffer solution (PBS) and distilled water, respectively, and fixed with 2.5% glutaralde-

hyde in 0.1M PBS for 1 h. After fixing, they were rinsed three times with 0.1M PBS for 10 min. The samples were then dehydrated in a graded series of alcohol (50, 75, 90, and 100%) for 10 min and subsequently dried by supercritical point CO₂. The dehydrated samples were sputter-coated with gold for SEM examination. The morphology of TiO₂ nanotubes as well as that of the adhered cells were observed using SEM (Quanta 600, FEI), FE-SEM (Phillips XL-30, FEI), and TEM (JEOL 200CX operated at 200 KV). In the quantitative assay, the adhered cells on sample surface were counted from back-scattered SEM images. For each type of samples, two substrates of each experimental condition and five locations from each substrate surface were used and photographed to obtain the data.

Trypan blue exclusion assay²¹

To count the number of viable cells, the trypan blue exclusion assay was carried out. After specific incubation periods, the adhered cells on the substrates were detached from the samples by trypsin-EDTA solution (Invitrogen, Carlsbad, CA). The solution including the detached cells was centrifuged at 1000 rpm for 10 min and removed by suction. The detached cells on each sample were stained with trypan blue dye agent (Invitrogen) at room temperature for 5 min. The stained cells were transferred in hemacytometer and counted by using optical microscope (Leica DM IRB, McBain Instruments, Chatsworth, CA). The viable cell density was calculated from the total counted number of viable cells divided by sample area.

MTT (3-(4,5-dimethylthiazole-2-yl)-2,5-diphenyl tetrazolium bromide) assay²²

To estimate the density of viable cells, MTT assay was employed. After the selected incubation periods, the samples were washed by PBS and transferred to a new 12-well polystyrene culture plate. MTT dye agent (1 mL; Sigma, St. Louis, MO) was added to each well. After 3 h of incubation in 5% CO₂ incubator, 1 mL of isopropanol was added to each well and the polystyrene plate was shaken for 30 min. After waiting for 30 min, the absorbance of each solution was measured at the wavelength of 570 nm with the subtraction of the 650 nm background by spectrophotometer (Biomate[®] 3, Thermo Electron, Madison, WI).

Alkaline phosphatase activity test^{23,24}

To measure the proliferation of cells cultured on the substrate, alkaline phosphatase (ALP) activity test was carried out. After the selected incubation periods, the samples were washed by PBS and transferred to a new 12-well polystyrene culture plate. Triton X-100 (500 μL of 0.1%; Sigma) was added to each well to study lysis of the cells. After incubating in 5% CO₂ incubator for 2 h, the solutions were transferred (2 mL) to a micro centrifuge tube and frozen at -80°C

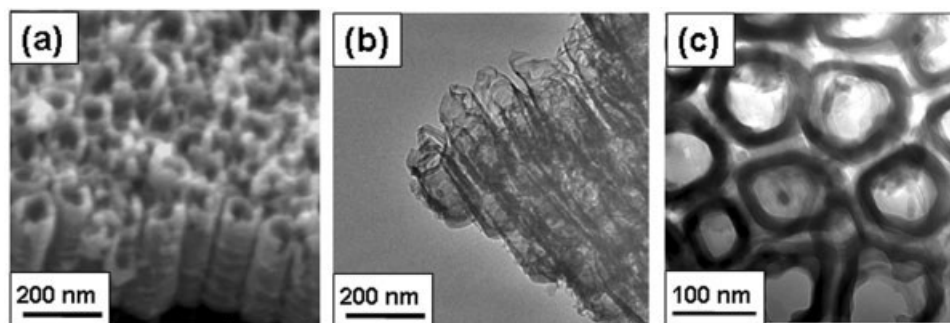


Figure 1. Structure of the vertically aligned TiO₂ nanotubes on Ti: (a) SEM micrograph, (b) TEM micrograph, and (c) cross-sectional TEM.

for 2 h. After 3 times freezing-thawing cycles to homogenize the solutions, aliquots of the solutions were used for measuring protein content (Bradford protein assay kit, Bio-Rad Laboratories, Hercules, CA) and 350 μ L of the solutions were used for ALP activity test. ALP substrate solution (350 μ L; ELPN-500, Bio-Assay Systems, Hayward, CA) was added to each solution and the solutions were mixed at room temperature for 30 min. After 30 min, 350 μ L of 1M NaOH was added to stop the reaction. The absorbance of each solution was measured at the wavelength of 405 nm by spectrophotometer.

RESULTS AND DISCUSSION

Morphology of TiO₂ nanotubes

Shown in Figure 1 are the microstructures of TiO₂ nanotubes prepared in the form of tightly adhered layer on Ti surface by anodization. The bond strength on Ti appears to be high, as it was very difficult to break off the TiO₂ nanotube layer by scratching or bending of the Ti underlayer, and a tensile loading of \sim 1700 psi (11.7 MPa) applied to the sample using epoxy bonded weight failed to break the TiO₂-Ti interface. Figure 1(a) is an SEM micrograph depicting the vertically aligned nature of the nanotubes on Ti metal substrate. The typical dimension of the hollow TiO₂ nanotubes is on the average \sim 100 nm outer diameter and \sim 70 nm inner diameter with \sim 15 nm in wall thickness, and \sim 250 nm in height, as is evident in the SEM micrograph of Figure 1(a), the TEM micrographs of Figure 1(b) (longitudinal view), and Figure 1(c) (cross-sectional view). While there are some variations of the nanotube diameter from location to location with the outer diameter ranging from \sim 70 to \sim 120 nm, the long-range overall distribution of nanotubes is more or less uniform. To transform the amorphous structure in the as-anodized nanotubes into a crystalline phase, a heat treatment process was employed. The heat-treated TiO₂ nanotube material (500°C/2 h in air) formed on Ti surface was found to

have anatase crystalline phase by glancing angle x-ray diffractometer analysis in agreement with previous research.²⁵ The anatase phase is known to be much more beneficial for bone growth than other phases such as the rutile phase of TiO₂ presumably because of the better lattice match with hydroxyapatite.²⁶

Morphology of adherent osteoblast

Figure 2 shows comparative SEM micrographs of MC3T3-E1 cells cultured on (a) pure Ti and (b) TiO₂ nanotubes after 2 h of incubation. The osteoblast cells cultured on Ti surface still remained in their original round shape, whereas the cells cultured on TiO₂ nanotubes attached on the surface and started to spread by filopodia [arrows in Fig. 2(b)]. It is well known that pure Ti forms a few nanometer thick, native TiO₂ passivation layer (responsible for good corrosion resistance of Ti),²⁷ which eventually causes the adhesion of osteoblastic cells, albeit at a much slower speed than the nanotube surface investigated in this work. It took \sim 12 h for a noticeable adhesion

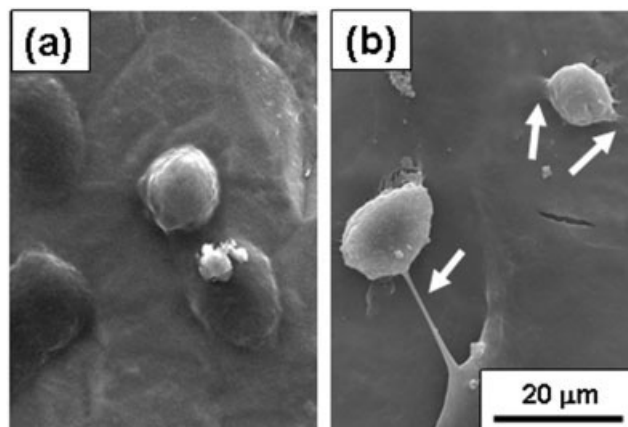


Figure 2. SEM micrographs of MC3T3-E1 osteoblast cells on (a) pure Ti and (b) TiO₂ nanotubes after 2 h of incubation.

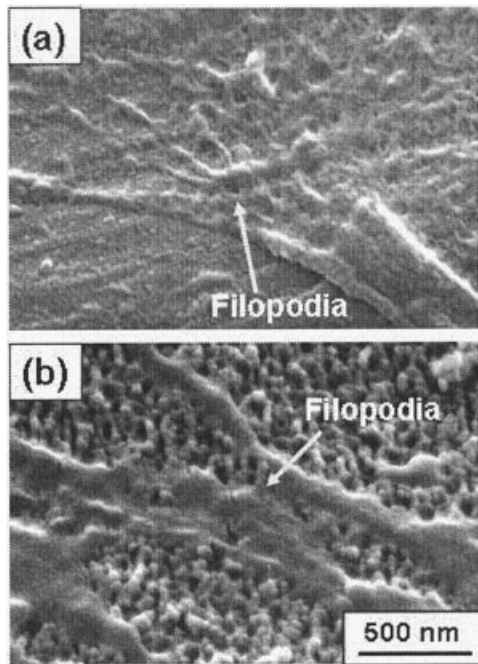


Figure 3. SEM micrographs showing osteoblast filopodia growth on (a) Ti surface (after 12 h) and (b) TiO₂ nanotube surface (after 2 h).

and propagation of the osteoblast cells to take place on Ti, as shown in Figure 3(a), as compared to less than a few hours for the nanotube surface. The growths of cells and propagation of filopodia are compared for the Ti sample [Fig. 3(a)] *versus* the TiO₂ nanotubes [Fig. 3(b)] after 12 and 2 h of incubation, respectively. It should be noted, however, that Figures 2 and 3 represent the spreading of filopodia from a single cell, not the division and proliferation of the number of cells that becomes more obvious after about one day of culture. This aspect of cell number proliferation is discussed later.

As discussed earlier, micrometer-sized bioactive materials (such as a hydroxyapatite layer coated on Ti surface) tend to exhibit interfacial failures. The nanoscaled bioactive materials such as the nanostructured hydroxyapatite²⁰ or the aligned TiO₂ nanostructures incorporated in this investigation form strongly bonded and stable nanoporous layer, which can reduce interfacial fracture. Natural bone is also composed of nanophase hydroxyapatite (~100 nm size regime) in the collagen matrix.²⁸ It is well known that fibroblast cells are more likely to attach on smooth surface layer in contrast to the osteoblastic cells, which can attach well on rough surface.⁷ Once an opportunity and time is given for the fibrous tissues to form at the boundary interface between the implant and the growing bone, these tissues keep osteoblast from adhering onto the surface of Ti implant, causing the undesirable loosening of the Ti implant. A rapid and strong adhesion of osteoblast on implant surface is

therefore an essential factor for successful bone growth. A nanostructured material, such as the natural bone, has a larger surface area and more frequent topographical changes than microscaled coating layer, and hence the chance of the fibroblast cells interfering with the bone growth at the interface is much reduced.

It is noteworthy that the TiO₂ nanotube structure of Figure 1 is not continuous, but is discrete [see Fig. 1(c)] with a gap between adjacent nanotubes of ~15 nm. Such a sub-division of a layer structure is important for minimizing the interfacial stresses between two dissimilar materials joined together, for example, often caused by growth-related stresses during deposition of the coating layer, by different crystal structure and lattice parameter, and by substantially different coefficient of thermal expansion of the substrate material and the growing layer material. It is experimentally confirmed, albeit qualitatively, that the vertically aligned TiO₂ nanotubes are strongly adherent to the Ti metal base, as it was very difficult to remove the nanotubes from the Ti surface by attempting to scrape off or by bending of the Ti substrate.

In addition to the advantages in mechanical properties, the gaps present between adjacent TiO₂ nanotubes may also be useful as a pathway for continuous supply of the body fluid with ions, nutrients, proteins, hormones, etc. This is likely to contribute positively to the health of the growing cells. In the absence of such pathways, the proliferating cells will eventually completely cover the bioactive implant material surface, and the bottom surface of the growing osteoblast cells would then have very limited access to body fluid.

Presented in Figure 4(a,b) are SEM micrographs showing the growth and adhesion of the osteoblast cells (after 2 h) on vertically nanoporous TiO₂ nanotubes. The micrographs seem to indicate that the filopodia of propagating osteoblast cells actually go into the vertical nanopores of the TiO₂ nanotubes. The observed rapid adherence and spread of osteoblastic cells cultured on TiO₂ nanotubes could be caused by three reasons. First, vertically aligned TiO₂ nanotubes exhibit enormously larger surface areas than the flat Ti surface. Second, the pronounced vertical topology contributes to the interlocked cell configuration. Third, it is speculated that the pathway in-between TiO₂ nanotube arrays can allow the passage of body fluid and act as the supply/storage route of nutrient, which is an essential biological element for cell growth.

Osteoblast adhesion and proliferation

Figure 5 represents the comparative back-scattered SEM micrographs of the cells cultured on (a) pure Ti, (b) amorphous TiO₂ nanotubes, and (c) anatase TiO₂

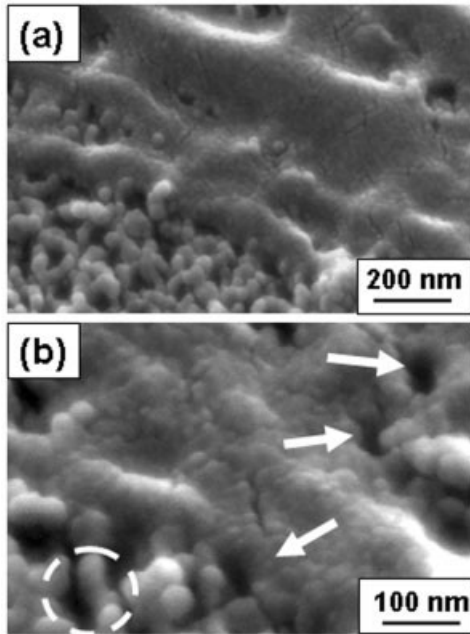


Figure 4. a: Micrograph showing the growth and adhesion of the osteoblast cells (after 2 h) on vertically nanoporous TiO₂ nanotubes. b: Higher magnification SEM. The circle indicates the TiO₂ nanotube and the arrows show the cell growth into nanotube pores.

nanotubes after 48 h of incubation. It is evident that the MC3T3-E1 cells adhesion and growth is significantly accelerated on TiO₂ nanotubes. The plot of the number of adhered cells as a function of culture pe-

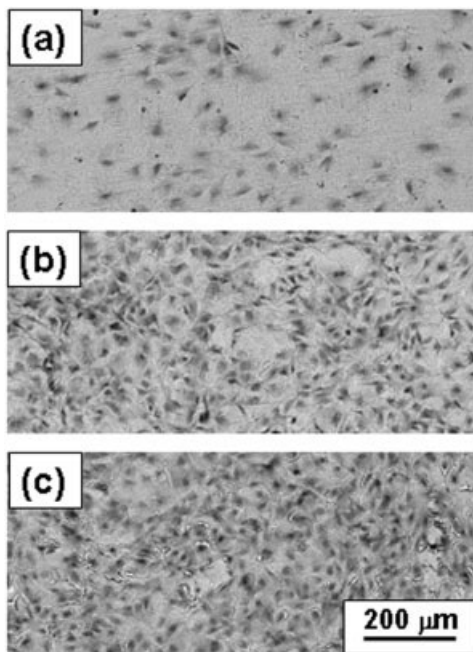


Figure 5. Comparative back-scattered SEM images of growing osteoblast cells on the surface of (a) Ti, (b) amorphous TiO₂ nanotubes, and (c) anatase TiO₂ nanotubes (after 48 h incubation).

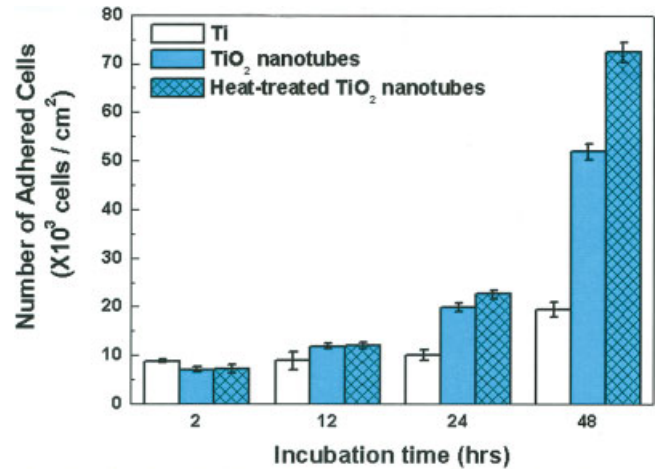


Figure 6. Number of adhered cells as a function of incubation period on the surface of Ti, amorphous TiO₂ nanotubes, and heat-treated (anatase) TiO₂ nanotubes. The error bars in the figure represent the standard deviation for six samples for each data. [Color figure can be viewed in the online issue, which is available at www.interscience.wiley.com.]

riod (Fig. 6) clearly confirms this trend, with the speed of cell adhesion and growth on anatase TiO₂ nanotubes being significantly higher after 48 h culture, by as much as ~300–400% as compared to the Ti surface. It is noted that at the early stage, e.g., after 2–12 h incubation, there was no difference in the data among the three surfaces investigated, as it is observed that a noticeable osteoblast cell proliferation has not occurred within ~12 h. However, the number of attached cells on the TiO₂ nanotubes markedly increases as the culture time is extended to 24 and 48 h. It is not clear why the amorphous TiO₂ nanotubes provide slightly reduced cell proliferation rate than the anatase TiO₂. Residual fluorine within the pores of unannealed amorphous nanotubes (introduced during the HF anodization process) might be a factor; however, further studies are required to clearly understand the cause for the observed difference in the cell behavior.

The trend shown in the SEM analysis data of Figure 6 is the same as shown in trypan blue exclusion assay (see Fig. 7), MTT assay (see Fig. 8), and ALP activity test (see Fig. 9). The cell count by SEM analysis and that by the trypan blue exclusion assay agrees reasonably well. The accelerated cell growth behavior obtained with TiO₂ substrate and measured by SEM and trypan blue exclusion assay is also reflected in the MTT assay and ALP activity test.

The accelerated growth of osteoblast cells observed here on vertically aligned nanotube surface may be useful for other applications, as it could be a useful route for accelerating cell proliferation of various other types of cells. For example, rare cells such as stem cells or disease cells of limited quantity may be cultured at a higher speed for therapeutic or diagnostic applications. Additional research in this respect is

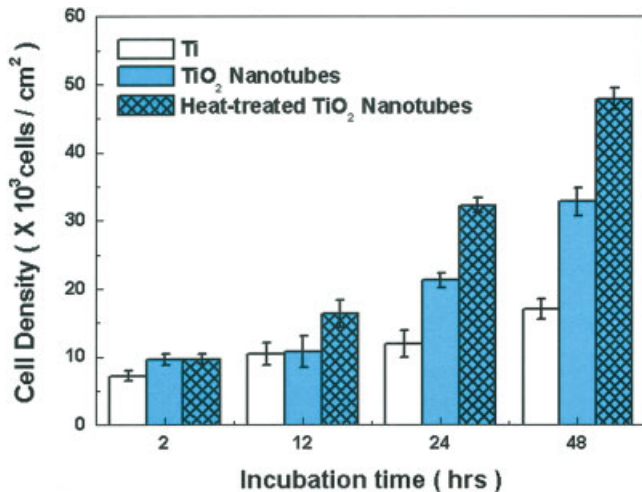


Figure 7. Trypan blue exclusion assay showing the density of adhered osteoblast cells cultured on polished Ti, amorphous TiO₂ nanotubes, and heat-treated (anatase) TiO₂ nanotubes after 2, 12, 24, and 48 h of incubation periods. The error bars in the figure represent the standard deviation for four samples for each data. [Color figure can be viewed in the online issue, which is available at www.interscience.wiley.com.]

being carried out, and the results will be reported in future publications.

CONCLUSION

In summary, the growth of MC3T3-E1 osteoblast cells on vertically aligned and laterally spaced tita-

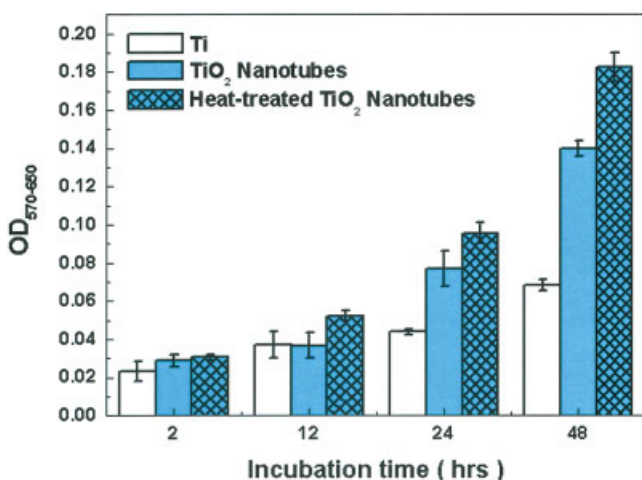


Figure 8. MTT assay data showing the optical density (OD) of reaction product of the MTT working solution with osteoblast cells cultured using polished Ti, amorphous TiO₂ nanotubes, and heat-treated (anatase) TiO₂ nanotubes after 2, 12, 24, and 48 h of incubation. The error bars in the figure represent the standard deviation for four samples for each data. [Color figure can be viewed in the online issue, which is available at www.interscience.wiley.com.]

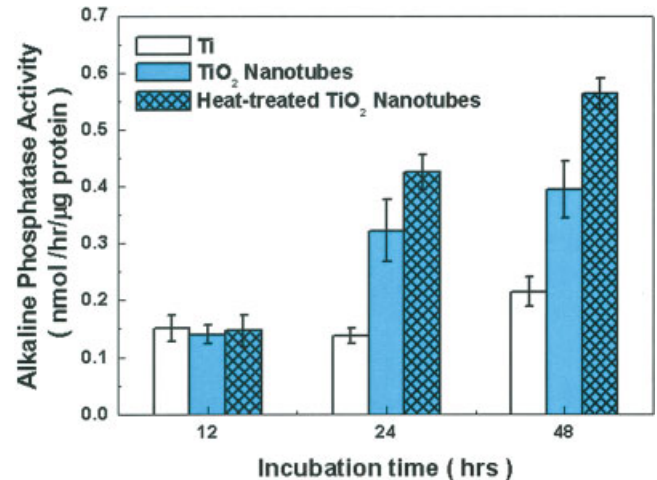


Figure 9. ALP activity of MC3T3-E1 osteoblast cells cultured on polished Ti, amorphous TiO₂ nanotubes, and heat-treated (anatase) TiO₂ nanotubes after 12, 24, and 48 h of incubation. The error bars in the figure represent the standard deviation for four samples for each data. [Color figure can be viewed in the online issue, which is available at www.interscience.wiley.com.]

nium oxide nanotubes on Ti surface has been investigated. It is demonstrated that the adhesion/propagation of the osteoblast cells is significantly improved by the topography of the nanotubes with the filopodia of the growing cells actually going into the nanotube pores, producing a interlocked cell structure. The number of the adhered cells on the TiO₂ nanotubes increases significantly by ~300–400% as compared to the cells adhering to the Ti metal surface, which is most likely caused by the pronounced topological feature, significantly increased surface area, and possibly the pathways for fluid present between the nanotubes. Such an array of vertical TiO₂ nanotubes well adherent on Ti implant surface can be useful as an excellent bioactive surface layer for orthopaedic and dental applications as the cell adhesion and bone growth on implant surface can be significantly accelerated. The aligned nanotube configuration may be a useful route for accelerating cell proliferation for various other types of cells.

The authors thank J. Blackwell at UC San Diego for helpful discussions and assistance in experiments.

References

- Linder L, Carlsson A, Marsal L, Bjursten LM, Branmark PI. Clinical aspects of osseointegration in joint replacement. *J Bone Joint Surg [Br]* 1988;70:550–555.
- Satomi K, Alagawa Y, Nikai H, Tsuru H. Bone-implant interface structures after nontapping and tapping insertion of screw-type titanium alloy endosseous implants. *J Prosthet Dent* 1988;59: 339–342.

3. Pillar RM, Lee JM, Maniopoulos C. Observation on the effect of movement on bone ingrowth into porous-surfaced implants. *Clin Orthop Rel Res* 1986;208:108–113.
4. Feng B, Weng J, Yang BC, Qu SX, Zhang XD. Characterization of surface oxide films on titanium and adhesion of osteoblast. *Biomaterials* 2003;24:4663–4670.
5. Puleo DA, Holleran LA, Doremus RH, Bizios R. Osteoblast response to orthopedic implant materials in vivo. *J Biomed Mater Res* 1989;25:711–723.
6. Satsangi A, Satsangi N, Glover R, Satsangi RK, Ong JL. Osteoblast response to phospholipid modified titanium surface. *Biomaterials* 2003;24:4585–4589.
7. Salata OV. Applications of nanoparticles in biology and medicine. *J Nanobiotech* 2004;2:3.
8. Shirkhanzadeh M. Bioactive calcium phosphate coating prepared by electrodeposition. *J Mat Sci Lett* 1991;10:1415–1417.
9. de Groot K, Geesink R, Klein CPAT, Selektion P. Plasma sprayed coating of hydroxyapatite. *J Biomed Mater Res* 1987;21:1375–1381.
10. Cotell CM, Chrisey DB, Graowsku KS, Spreue JA. Pulsed laser deposition of hydroxyapatite thin films of Ti6Al4V. *J Appl Biomater* 1992;8:87–92.
11. Ong JL, Lucas LC, Lacefield WR, Rigney ED. Structure, solubility and bond strength of thin calcium phosphate coatings produced by ion beam sputter deposition. *Biomaterials* 1992;13:249–254.
12. Kokubo T, Miyaji F, Kim HM, Nakamura T. Spontaneous apatite formation on chemically treated titanium metals. *J Am Ceram Soc* 1996;79:1127–1129.
13. Weng W, Baptista JL. Sol-gel derived porous hydroxyapatite coating. *J Mater Sci Mater Med* 1998;9:159–163.
14. Yang CY, Wang BC, Lee TM, Chang E, Chang GL. Intramedullary implant of plasma-sprayed hydroxyapatite coating: An interface study. *J Biomed Mater Res* 1997;36:39–48.
15. Webster TJ, Ergun C, Doremus RH, Siegel RW, Bizios R. Enhanced functions of osteoblast on nanophase ceramics. *Biomaterials* 2000;21:1803–1810.
16. Webster TJ, Schandler LS, Siegel RW, Bizios R. Mechanisms of enhanced osteoblast adhesion on nanophase alumina involve vitronectin. *Tissue Eng* 2001;7:291–301.
17. Lakshmi BB, Patrisi CJ, Martin CR. Sol-gel template synthesis of semiconductor oxide micro- and nanostructures. *Chem Mater* 1997;9:2544–2550.
18. Miao Z, Xu D, Ouyang J, Guo G, Zhao X, Tang Y. Electrochemically induced sol-gel preparation of single-crystalline TiO₂ nanowires. *Nano Lett* 2002;2:717–720.
19. Gong D, Grimes CA, Varghese OK, Hu W, Singh RS, Chen Z, Dickey EC. Titanium oxide nanotube arrays prepared by anodic oxidation. *J Mater Res* 2001;16:3331–3334.
20. Oh SH, Finones R, Chen LH, Jin S. Growth of nano-scale hydroxyapatite using chemically treated titanium oxide nanotubes. *Biomaterials* 2005;26:4938–4943.
21. Uchida M, Oyane A, Kim HM, Kokubo T, Ito A. Biomimetic coating of laminin-apatite composite on titanium metal and its excellent cell-adhesive properties. *Adv Mater* 2004;16:1071–1074.
22. Mosmann T. Rapid colorimetric assay for cellular growth and survival: Application to proliferation and cytotoxicity assays. *J Immunol Methods* 1983;65:55–63.
23. Dolder J, Bancroft GN, Sikavitsas VI, Spauwen PHM, Jansen JA, Mikos AG. Flow perfusion culture of marrow stromal osteoblasts in titanium fiber mesh. *J Biomed Mater Res A* 2003;64:235–241.
24. Declercq HA, Verbeeck R, De Ridder R, Schacht EH, Cornelissen MJ. Isolation, proliferation and differentiation of osteoblastic cells to study cell/biomaterial interactions: Comparison of different isolation technique and source. *Biomaterials* 2005;26:4964–4974.
25. Varghese OK, Gong D, Paulose M, Grimes CA, Dickey EC. Crystallization and high-temperature structural stability of titanium oxide nanotube arrays. *J Mater Res* 2003;18:156–165.
26. Uchida M, Kim HM, Kokubo T, Fujibayashi S, Nakamura T. Structural dependence of apatite formation on titania gels in a simulated body fluid. *J Biomed Mater Res* 2003;64:164–170.
27. Feng B, Chen JY, Qi SK, He L, Zhao JZ, Zhang XD. Characterization of surface oxide films on titanium and bioactivity. *J Mater Sci Mater Med* 2002;13:457–464.
28. Kaplan FS, Hayes WC, Keaveny TM, Boskey A, Einhorn TA, Iannotti JP. In: Simon SR, editor. *Orthopaedic Basic Science*. Ohio: American Academy of Orthopedic Surgeons; 1994. p 127–185.